ACS APPLIED MATERIALS & INTERFACES

Research Article

www.acsami.org

Origin of the Accumulation Layer at the InN/a-In_2O_3 Interface

Antonio Aliano,[†] Giancarlo Cicero,*[,†,‡] and Alessandra Catellani[‡,¶]

[†]Department of Applied Science and Technology, Politecnico di Torino, Corso Duca degli Abruzzi 24, 10129 Torino, Italy

[‡]CNR-IMEM, Parco Area delle Scienze, 37A, I-43010 Parma, Italy

[¶]CNR-NANO, Istituto Nanoscienze, Centro S3, I-41125 Modena, Italy

ABSTRACT: We perform first-principles Density Functional Theory calculations for the amorphous In_2O_3/InN $(1\bar{1}00)$ heterostructure. Our results suggest that the interface between InN and its native amorphous oxide is a type "I" interface as observed in X-ray photoemission spectroscopy data for the same materials in the crystalline form. The microscopic analysis of the system reveals the presence of peculiar structural features localized at the interface, such as the formation of N−O bonds and the existence of N dangling bonds, that are responsible for donor states. These findings shed light on the origin of the electron accumulation layer occurring at the interface in spontaneously oxidized InN nanowires, recently associated with the observed increase in conductivity for such systems.

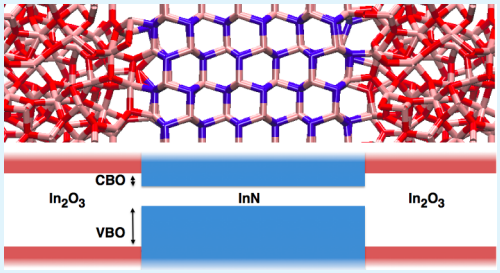

KEYWORDS: *DFT, interface, native oxide, heterostructure, InN*

1. INTRODUCTION

Indium nitride (InN), an exemplar III-nitride semiconductor, and its native oxide (In_2O_3) have become key materials for a wide variety of electronic and optoelectronic technologies in both thin films and nanostructured forms.[1−3] In the last several years, wurtzite InN nanostructures have been developed for sensors or new generation solar cells[4,5] while amorphous indium oxide has been used as a promising component in transparent and flexible electronic devices[6] further widening the frontiers of their applications. The heterojunction between these two materials has been the subject of recent studies since it can be employed as a basic element in high frequency field effect transistors.[7] Furthermore, indium oxide spontaneously forms at the InN surfaces when exposed to air.[5,8−11] The formation of this indium oxide coating at InN nanowire (NW) walls is critical for applications: An oxidation shell is a desired protection against thermal dissociation of InN in nanocables;[12] furthermore, it has been recently supposed that this very thin (<10 Å) In_2O_3 layer may act as a confining barrier for the formation of a bidimensional electron accumulation layer at the NW lateral walls, believed to be a determinant for the observed increase of the InN NW conductivity.[5] The increase of conductivity upon formation of an interface, and in the presence of an oxide, namely, a compound with a larger band gap than the pristine material, is an intriguing experimental result that still awaits for a theoretical investigation.[5]

In order to shed some light on this puzzle, we performed *ab initio* simulations of the InN/In_2O_3 interface. *Ab initio* calculations stand out as a powerful theoretical tool for the atomic scale investigations of materials, and in the case of indium based systems, they gave a decisive contribution in the study of InN surfaces[13−15] and in the interpretation of experimental studies of crystalline and amorphous In_2O_3.[16−19] Recently, also, the band energy offsets for the crystalline heterojunction have been assessed on the basis of quasi-particle methods; interface effects, however, were not taken into account explicitly.[20]

Hereafter, we consider a realistic atomistic model to represent the InN/In_2O_3 interface in spontaneously oxidized InN NWs. Since the most common morphology of InN NW facets is the one exposing the $(1\bar{1}00)$ nonpolar surface,[5] we deal with the InN $(1\bar{1}00)$ surface in contact with the amorphous indium oxide (a-In_2O_3) structure. In the absence of well-defined information on the interface between InN and its native oxide, we first perform simulations on the initial InN oxidation in terms of oxygen potential energy surface (PES) to obtain an unbiased choice for the position of oxygen atoms of the amorphous phase on the InN substrate. We then study the electronic properties of the InN/In_2O_3 heterojunction. Our calculations show that this heterostructure presents a type I band alignment, with the indium oxide valence band edge being lower in energy than the InN one. Moreover, the interface is characterized by defects such as dangling bonds at the interfacial nitrogen atoms which generate filled defect states at the Fermi level, imparting local metallic character to the interface. The presence of such donor states is consistent with the formation of an electron accumulation layer at the interface, in agreement with recent experimental observation.[5]

2. METHOD

The calculations were performed within the *ab initio* Density Functional Theory (DFT) using ultrasoft pseudopotentials[21] in the Perdew−Burke−Ernzerhof (PBE[22]) approximations as implemented

Received: December 21, 2014
Accepted: February 18, 2015
Published: February 18, 2015

DOI: 10.1021/am508944s
ACS Appl. Mater. Interfaces 2015, 7, 5415−5419

in the QUANTUM ESPRESSO package.[23] A plane waves basis set was used to expand wave functions (charge density) with a cutoff in energy of 30 Ry (300 Ry).

Two different sets of calculations were performed: First, we calculated the potential energy surface (PES) for an oxygen adatom on the InN $(1\bar{1}00)$ plane, in order to estimate how the adsorption energy varies as a function of the adsorption site (see Figure 1). These

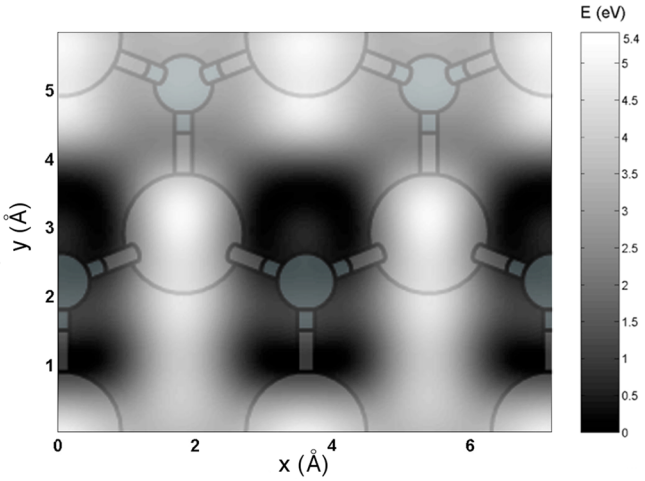

Figure 1. Potential energy surface for an oxygen adatom on the InN $(1\bar{1}00)$ surface: The top view of the underlying surface is reproduced as blue/small (N) and gray/large (In) spheres. The lowest energy configuration is taken as reference and set to zero of the energy scale.

calculations were performed in a (1×1) surface supercell containing 12 layers of an InN slab showing $(1\bar{1}00)$ facets and ∼10 Å vacuum. The electronic properties were evaluated using a $(8 \times 8 \times 1)$ k-point regular grid. In the absence of well-defined experimental data, this simulation allowed us to define in an unbiased way the optimal choice (lowest energy positions) for the oxygen atoms of the amorphous phase on the InN surface.

We then built the model interface: The initial configurations of the InN/In_2O_3 interface were obtained by merging a 12 layer InN slab (∼16.7 Å thick) showing $(1\bar{1}00)$, 3×2 surface facets and an a-In_2O_3 sample (∼11.3 Å thick)[24] obtained by *ab initio* molecular dynamics.[18] The lateral dimensions of the amorphous sample are chosen to be commensurate with the InN-3×2 surface. This interface supercell was set to be periodic along the direction perpendicular to the heterojunction (*c* lattice parameter), and the optimal distance between the two materials was determined by varying *c* to achieve the minimum energy structure; a sketch of the interface supercell is reproduced in Figure 2. The relative position of the a-In_2O_3 layer with respect to the InN slab at the interface was defined by considering the minimum energy system for the interaction of a single oxygen atom at the clean InN surface, as described above. The large supercell size allowed the use of the Γ point only to integrate over the Brillouin zone.[25] Atomic relaxation was considered to be converged when forces were smaller than 26 meV/Å. After energy minimization, the electronic properties were calculated using a $(3 \times 3 \times 1)$ k-mesh grid within the PBE + *U* scheme, for a better description of the d-shell of the indium atom: The Hubbard *U* corrections were introduced to the d states (U_d = 6.0 eV) of In and to the p orbitals of the anions (N, U_p^N = 1.5 eV, and O, U_p^O = 3.0 eV) similarly to the parametrization used in InN[13,26] and bcc In_2O_3.[27]

In order to provide an unbiased description of the crystalline/amorphous interface, that is intrinsically hard to define, we considered four different amorphous configurations.[28] In this way, we collected information on the structural and electronic properties of 8 independent buried interfaces (two in each supercell), that allowed us to meaningfully sample the phase space.

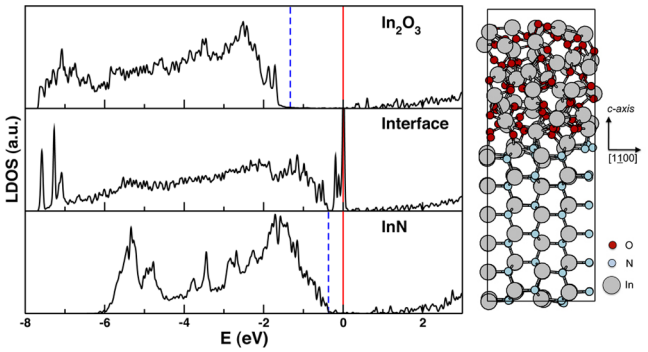

Figure 2. (Left Panel) Local density of states (LDOS) at the PBE + *U* level of an a-In_2O_3/InN $(1\bar{1}00)$ interface as obtained for a representative calculation. The different panels show from top to bottom the projection of DOS on the different portions of the slab, namely, the bulk-like a-In_2O_3, the interfacial zone, and the bulk-like InN DOS. The zero for the energy scale is set at the Fermi level of the heterostructure system (red line). Dotted blue lines indicate the a-In_2O_3 and wurtzite InN valence band maximum (VBM) obtained after alignment of the In-4d states of bulk calculations. (Right Panel) Side view of the a-In_2O_3/InN heterostructure in the simulated unit cell. The unit cell contains 116 In (gray spheres), 66 O (red spheres), and 72 N (blue spheres) atoms.

3. RESULTS AND DISCUSSION

In the following, we first discuss the potential energy surface for the adsorption of an oxygen atom at the clean InN $(1\bar{1}00)$ surface and describe how this information can be used to build the interface between In_2O_3 and InN $(1\bar{1}00)$; afterward, we present the structural features of the minimum energy In_2O_3/InN $(1\bar{1}00)$ heterostructure and discuss the implications of these features on the electronic properties of the system.

3.1. Initial Stages of InN $(1\bar{1}00)$ Surface Oxidation. The optimal configuration for oxygen adatoms on the crystalline InN nonpolar surfaces has been studied in terms of PES calculated by first-principles simulations: Results are reported in Figure 1, where we plot PES in eV on the (1×1) InN $(1\bar{1}00)$ surface. The most favorable adsorption site is represented by the darker areas of the figure, and it corresponds to an oxygen atom bound to a surface nitrogen atom of the InN substrate. In this configuration, nitrogen restores the 4-fold coordination, typical on bulk InN, forming three bonds with the indium atoms of the substrate and a short bond (1.30 Å long) with the oxygen adatom. The adsorption energy corresponding to this geometry is −1.33 eV. This large energy gain upon N−O bond formation is a marker of the bond strength and of the large affinity between N and O atoms. Indeed, In−N−O complexes are experimentally observed during the first stages of InN oxidation.[29] Formation of the N−O bonds is rather likely to occur also at the InN/a-In_2O_3 interface: For this reason, we maximized, when possible, the number of O atoms in the minimal PES positions, when matching the a-In_2O_3 and the InN slabs to form the initial interface structure (without modifying the amorphous sample). As discussed in the following, these NO bonds, that originate from the exposed O atoms in the amorphous surface, give rise to defect (interface) states that appear in the interface DOS.

3.2. In_2O_3/InN $(1\bar{1}00)$ Heterostructure. Once information on the initial stages of surface oxidation was achieved, we use the O stable sites to build a model interface between the nitride and its amorphous oxide, previously obtained by means of *ab initio* molecular dynamics simulations at finite temper-

DOI: 10.1021/am508944s
ACS Appl. Mater. Interfaces 2015, 7, 5415−5419

ature.[18] In order to gain a statistically meaningful description, we built different interfaces (4 different slabs, with different although equivalent amorphous geometries). We first relaxed the supercell lattice parameter perpendicular to the interface, in order to minimize the stress between the two compounds, and then let the overall system relax, until forces were lower than than 26 meV/Å.[28]

Despite the disordered atomic arrangement typical of an interface involving an amorphous material, some common structural features can be identified for all the analyzed InN $(1\bar{1}00)$/a-In_2O_3 systems. The two materials are preferentially connected through bonds between indium and nitrogen top layer atoms of the InN $(1\bar{1}00)$ surface and oxygen and indium atoms of the amorphous oxide, without formation of a relevant number of *wrong* bonds, involving atoms of the same species. To provide a quantitative estimate of the stability of our model interface structure, we calculated the interface energy for all the systems we considered. This is defined as the difference between the total energy of the supercell and that of the two bulk constituents. We obtain in this way an average value of interface energy of 0.90 ± 0.18 J/m^2. If compared to the surface energy of the clean InN $(1\bar{1}00)$ (before oxidation takes place), which was reported to be 1.5 J/m^2,[14] one can see that the comparison is fully compatible with the presence of stable interfaces and in agreement with the spontaneous formation of a native amorphous oxide layer on top of the InN surface, as observed experimentally.[29] Our results reveal that upon oxidation buckling of the In−N topmost dimers[14] is strongly reduced and a local bulk-like environment (coordination numbers, atomic arrangements) is restored beyond the first coordination shell of the atoms at the interface.

Together with these features, some structural localized peculiarities can be indentified: (i) in 4 out of the 8 interfaces here analyzed, it is possible to notice the formation of strong N−O bonds (d_{N-O} = 1.3−1.6 Å) corresponding to a concentration of about 2% of interfacial bonds; (ii) the irregularities of a-In_2O_3 structure allow the persistency of N unsaturated bonds at the interface; (iii) the O−O defect (d_{O-O} = 1.45 Å) existing in the initial a-In_2O_3 structure,[18] and responsible for the presence of defect states at the In_2O_3 valence band maximum (VBM), is still present after system relaxation.

It is thus interesting to analyze if these structural marks affect the electronic properties of the interface and to what extent. In Figure 2, we plot the density of states (DOS) of a representative supercell. In order to highlight the interface details, the local density of states (LDOS) for each part of the system is calculated by projecting the total DOS onto the atoms belonging to different portions of the slab: The InN part (bottom panel), the a-In_2O_3 (top panel), and the interface layers (central panel). The energy zero is set in the figure to the Fermi level (E_F, red continuous line) of the interface calculations.

In order to interpret the picture, to characterize interface energy levels, and to assign peculiar features in the density of states to the two subsystems forming the heterostructure, it is essential to determine a band lineup procedure, leading to the definition of the valence band offset (VBO). The identification of the Valence edges of InN and a-In_2O_3 from a direct analysis of the DOS is not straightforward. Here, we choose to define the valence band edges of the subsystems by comparing the features of the DOS projected on the atoms that have bulk-like structures (i.e., far from the interface) with those obtained from bulk calculations: In this case, we use the indium semicore d-levels, which are only slightly affected by the chemical environment. This procedure allows us to define the valence band maximum (VBM) for each constituent (dashed blue lines in Figure 2). Calling E_{sh}^{InN} and $E_{sh}^{a\text{-}In_2O_3}$ the energy shifts applied to the bulk DOS in order to match the position of the d states of the interface calculations, VBO can be calculated by employing the following formula:

$$\mathrm{VBO} = (E_{VBM}^{InN} - E_{sh}^{InN}) - (E_{VBM}^{a\text{-}In_2O_3} - E_{sh}^{a\text{-}In_2O_3}) \quad (1)$$

where E_{VBM}^{InN} and $E_{VBM}^{a\text{-}In_2O_3}$ represent the valence band maximum (VBM) for wurtzite InN and a-In_2O_3 bulk structures. Our results show that $E_{VBM}^{InN} > E_{VBM}^{a\text{-}In_2O_3}$ for all our model systems and that the VBO calculated through eq 1 averaged over the different interfaces studied is 1.05 ± 0.10 eV, depending on the structural details of the interface.

The conduction band offset (CBO) can be obtained by adding to the valence band top of InN and a-In_2O_3 the respective energy gaps. As shown in ref 13, the Hubbard correction improves the description of the electronic properties of the valence and conduction band of indium compounds but still underestimates the energy gap.[30] For this reason, we evaluated the CBO employing the experimental energy gap values, namely, ΔE_g^{InN} = 0.64 eV[1] and $\Delta E_g^{a\text{-}In_2O_3}$ = 2 eV.[31,32] Accordingly, the InN $(1\bar{1}00)$/a-In_2O_3 interface can be recognized as type I, presenting a straddling energy band lineup, with CBO of 0.35 eV evaluated as

$$\mathrm{CBO} = \Delta E_g^{a\text{-}In_2O_3} - \Delta E_g^{InN} - \mathrm{VBO} \quad (2)$$

where $\Delta E_g^{a\text{-}In_2O_3}$ and ΔE_g^{InN} are the energy gap of bulk a-In_2O_3 and wurtzite InN. These findings are in qualitative agreement with X-ray spectroscopic data measured for the same materials in the crystalline form.[33,34]

The DOS projected on the interface atoms and reported in the central panel of Figure 2 reveals the presence of a prominent peak at the Fermi level. This peak originates from structural details at the interface region such as N dangling bonds and N−O bonds, that give rise to filled defect states. The charge density pertaining to one of these states, namely, the highest occupied (HO), is depicted in Figure 3 which offers a close-up of the heterostructure, revealing that HO is indeed localized at the interface. These interface states act as donors and impart local metallic character to the interface. This result supports and complements the experimental observation[5] relative to the formation of an electron accumulation layer at the oxidized walls of InN nanowires.

4. CONCLUSIONS

In conclusion, our first-principles calculations performed for the InN $(1\bar{1}00)$/a-In_2O_3 heterostructure provide an atomistic description of a nitride compound coupled with its native amorphous oxide. The energy band offsets reveal straddling energy level lineups predicting a type I interface as observed in X-ray spectroscopic experimental data for the same crystalline materials. The occupied interface states close to the Fermi level give a prominent contribution to the charge density in the InN conduction band: This result provides an interpretation to recent experimental data on the formation of an electron accumulation layer which strongly influences the electron transport properties in oxidized InN nanosystems.

DOI: 10.1021/am508944s
ACS Appl. Mater. Interfaces 2015, 7, 5415−5419

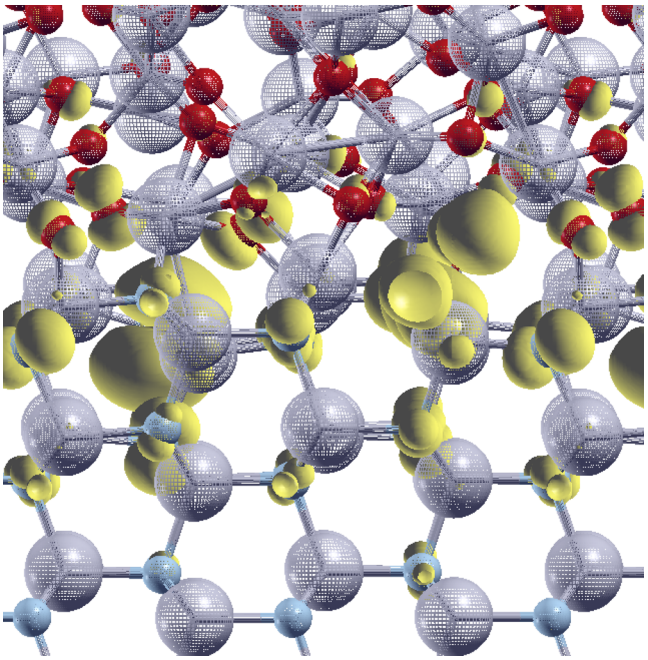

Figure 3. Charge density isocontour (yellow) of the highest occupied (HO) state at Γ. Gray spheres represent In atoms, while red (blue) spheres indicate O (N) atoms: The picture clearly shows that HO is localized at the interface.

AUTHOR INFORMATION

Corresponding Author

*Phone: +39 011 5644659. Fax: +39 011 5647399. E-mail: giancarlo.cicero@polito.it.

Notes

The authors declare no competing financial interest.

ACKNOWLEDGMENTS

The authors acknowledge funding from the European Union Seventh Framework Program under grant agreement ITN-Nanowiring (Grant No. 265073) and NANOLICHT project supported by the ERANET initiative NanoSci-ERA (within the EU FP6). We acknowledge the CINECA award under the ISCRA initiative and the Italian Institute of Technology for the availability of high performance computing resources and support.

REFERENCES

(1) Wu, J. When Group-III Nitrides Go Infrared: New Properties and Perspectives. *J. Appl. Phys.* **2009**, *106*, 011101.

(2) Klein, A.; Körber, C.; Wachau, A.; Süberlich, F.; Gassenbauer, Y.; Harvey, S. P.; Proffit, D. E.; Mason, T. O. Transparent Conducting Oxides for Photovoltaics: Manipulation of Fermi Level, Work Function and Energy Band Alignment. *Materials* **2010**, 3, 4892−4914.

(3) Cheng, G.; Stern, E.; Guthrie, S.; Reed, M. A.; Klie, R.; Hao, Y.; Meng, G.; Zhang, L. Indium Oxide Nanostructures. *Appl. Phys. A: Mater. Sci. Process.* **2006**, *85*, 233−240.

(4) Wright, J. S.; Lim, W.; Norton, D. P.; Pearton, S. J.; Ren, F.; Johnson, J. L.; Ural, A. Nitride and Oxide Semiconductor Nanostructured Hydrogen Gas Sensors. *Semicond. Sci. Technol.* **2010**, *25*, 024002.

(5) Werner, F.; Limbach, F.; Carsten, M.; Denker, C.; Malindretos, J.; Rizzi, A. Electrical Conductivity of InN Nanowires and the Influence of the Native Indium Oxide Formed at Their Surface. *Nano Lett.* **2009**, *9*, 1567−1571.

(6) Nomura, K.; Ohta, H.; Takagi, A.; Kamiya, T.; Hirano, M.; Hosono, H. Room-Temperature Fabrication of Transparent Flexible Thin-Film Transistors Using Amorphous Oxide Semiconductors. *Nature* **2004**, *432*, 488−492.

(7) Wang, C. Y.; Cimalla, V.; Lebedev, V.; Kups, T.; Ecke, G.; Hauguth, S.; Ambacher, O.; Lozano, J. G.; Morales, F. M.; González, D. InN/In_2O_3 Heterostructures. *Phys. Status Solidi C* **2008**, *5*, 1627−1629.

(8) Sarantopoulou, E.; Kollia, Z.; Dražic, G.; Kobe, S.; Antonakakis, N. S. Long-term Oxidization and Phase Transition of InN Nanotextures. *Nanoscale Res. Lett.* **2011**, *6*, 387.

(9) Lee, I. J.; Yu, C.; Shin, H.-J.; Kim, J.-Y.; Lee, Y. P.; Hur, T.-B.; Kim, H.-K. Oxidation Study of Polycrystalline InN Film Using in Situ X-ray Scattering and X-ray Photoemission Spectroscopy. *Thin Solid Films* **2007**, *515*, 4691−4695.

(10) Lozano, J. G.; Morales, F. M.; García, R.; González, D.; Lebedev, V.; Wang, C. Y.; Cimalla, V.; Ambacher, O. Cubic InN Growth on Sapphire (0001) Using Cubic Indium Oxide as Buffer Layer. *Appl. Phys. Lett.* **2007**, *90*, 091901.

(11) Lebedev, V.; Wang, Y. C.; Hauguth, S.; Polyakov, V.; Schwierz, F.; Cimalla, V.; Kups, T.; Morales, F. M.; Lozano, J. G.; González, D.; Himmerlich, M.; Schaefer, J. A.; Krischok, S.; Ambacher, O. Electron Transport Properties of Indium Oxide-Indium Nitride Metal-Oxide-Semiconductor Heterostructures. *Phys. Status Solidi C* **2008**, *5*, 495−498.

(12) Zhang, J.; Jiang, F.; Yang, Y.; Xu, B.; Li, J.; Wang, X.; Wang, S. Growth and Structural Characterization of InN/In_2O_3 Coaxial Nanocables. *Mater. Lett.* **2006**, *60*, 2153−2157.

(13) Terentjevs, A.; Catellani, A.; Prendergast, D.; Cicero, G. Importance of On-site Corrections to the Electronic and Structural Properties of InN in Crystalline Solid, Nonpolar Surface, and Nanowire Forms. *Phys. Rev. B* **2010**, *82*, 165307.

(14) Terentjevs, A.; Cicero, G.; Catellani, A. First-Principles Investigations of InN Nonpolar Surface Functionalization. *J. Phys. Chem. C* **2009**, *113*, 11323−11328.

(15) Van de Walle, C. G.; Segev, D. Microscopic Origins of Surface States on Nitride Surfaces. *J. Appl. Phys.* **2007**, *101*, 081704.

(16) King, P. D. C.; Veal, T. D.; Fuchs, F.; Wang, C. Y.; Payne, D. J.; Bourlange, A.; Zhang, H.; Bell, G. R.; Cimalla, V.; Ambacher, O.; Egdell, R. G.; Bechstedt, F.; McConville, C. F. Band Gap, Electronic Structure, and Surface Electron Accumulation of Cubic and Rhombohedral In_2O_3. *Phys. Rev. B* **2009**, *79*, 205211.

(17) Walsh, A.; Da Silva, J. L. F.; Wei, S.-H.; Körber, C.; Klein, A.; Piper, L. F. J.; DeMasi, A.; Smith, K. E.; Panaccione, G.; Torelli, P.; Payne, D. J.; Bourlange, A.; Egdell, R. G. Nature of the Band Gap of In_2O_3 Revealed by First-Principles Calculations and X-ray Spectroscopy. *Phys. Rev. Lett.* **2008**, *100*, 167402.

(18) Aliano, A.; Catellani, A.; Cicero, G. Characterization of Amorphous In_2O_3: An Ab Initio Molecular Dynamics Study. *Appl. Phys. Lett.* **2011**, *99*, 211913.

(19) Lany, S.; Zakutayev, A.; Mason, T. O.; Wager, J. F.; Poeppelmeier, K. R.; Perkins, J. D.; Berry, J. J.; Ginley, D. S.; Zunger, A. Surface Origin of High Conductivities in Undoped In_2O_3 Thin Films. *Phys. Rev. Lett.* **2012**, *108*, 016802.

(20) Schleife, A.; Fuchs, F.; Rödl, C.; Furthmüller, J.; Bechstedt, F. Branch-Point Energies and Band Discontinuities of III-Nitrides and III-/II-Oxides from Quasiparticle Band-Structure Calculations. *Appl. Phys. Lett.* **2009**, *94*, 012104.

(21) Vanderbilt, D. Soft Self-Consistent Pseudopotentials in a Generalized Eigenvalue Formalism. *Phys. Rev. B* **1990**, *41*, 7892−7895.

(22) Perdew, J. P.; Burke, K.; Ernzerhof, M. Generalized Gradient Approximation Made Simple. *Phys. Rev. Lett.* **1996**, *77*, 3865−3868.

(23) Giannozzi, P. QUANTUM ESPRESSO: A Modular and Open-Source Software Project for Quantum Simulations of Materials. *J. Phys.: Condens. Matter* **2009**, *21*, 395502.

(24) These dimensions allow one to reproduce electronic and structural properties of the InN $(1\bar{1}00)$ surface[13] and the structural properties, g(r), of the amorphous In_2O_3.[18]

DOI: 10.1021/am508944s
ACS Appl. Mater. Interfaces 2015, 7, 5415−5419

(25) Since we used a InN-3 × 2 surface supercell, the Γ point samples 3 × 2 k-points of the interface BZ, which is enough to get accurate electronic structure calculations of the system.
(26) Molina-Sanchez, A.; Garcia-Cristobal, A.; Cantarero, A.; Terentjevs, A.; Cicero, G. LDA+U and Tight-Binding Electronic Structure of InN Nanowires. *Phys. Rev. B* **2010**, *82*, 165324.
(27) Erhart, P.; Klein, A.; Egdell, R. G.; Albe, K. Band Structure of Indium Oxide: Indirect Versus Direct Band Gap. *Phys. Rev. B* **2007**, *75*, 153205.
(28) The relaxed *c* vectors values for the four supercells are 31.60, 32.57, 32.90, and 31.28 Å.
(29) Foley, C. P.; Lyngdal, J. Analysis of Indium Nitride Surface Oxidation. *J. Vac. Sci. Technol. A* **1987**, *5*, 1708−1712.
(30) The calculated energy gap of InN and In_2O_3 at the PBE+U level are about 0.1 and 1.0 eV, respectively.
(31) Ulutaş, K.; Değer, D.; Skarlatos, Y. Thickness Dependence of Optical Properties of Amorphous Indium Oxide Thin Films Deposited by Reactive Evaporation. *Phys. Status Solidi A* **2006**, *203*, 2432−2437.
(32) The reduced band gap of the amorphous phase with respect to the bixbyte phase is mostly due to band tailing effects as highlighted in ref 18.
(33) Eisenhardt, A.; Eichapfel, G.; Himmerlich, M.; Knübel, A.; Passow, T.; Wang, C.; Benkhelifa, F.; Aidam, R.; Krischok, S. Valence Band Offsets at Oxide/InN Interface Determined by X-ray Photoelectron Spectroscopy. *Phys. Status Solidi C* **2012**, *9*, 685.
(34) Song, H. P.; Yang, A. L.; Wei, H. Y.; Guo, Y.; Zhang, B.; Zheng, G. L.; Yang, S. Y.; Liu, X. L.; Zhu, Q. S.; Wang, Z. G.; Yang, T. Y.; Wang, H. H. Determination of Wurtzite InN/Cubic In_2O_3 Heterojunction Band Offset by X-ray Photoelectron Spectroscopy. *Appl. Phys. Lett.* **2009**, *94*, 222114.

DOI: 10.1021/am508944s
ACS Appl. Mater. Interfaces 2015, 7, 5415−5419